Process Boundary Approach to Separations Synthesis

Thomas G. Pressly and Ka M. Ng
Dept. of Chemical Engineering, University of Massachusetts, Amherst, MA 01003

A method for synthesizing separation processes for multicomponent mixtures is presented which identifies the regions, boundaries, and the lower dimensional varieties in an N-dimensional space. Both thermodynamic and equipment boundaries, which may block or limit a proposed separation step, are considered. To facilitate process synthesis, process boundaries are approximated as linear hyperplanes if appropriate, while nonlinear boundaries are represented using a set of linear hyperplanes. In conjunction with the available separation task selection methods, a step-by-step procedure is proposed to generate complete flowsheet alternatives, which allow bypassing both thermodynamic and equipment boundaries to achieve a given separations objective. Several example problems are solved using a spreadsheet program to illustrate the simplicity and applicability of this approach.

Introduction

Separation system synthesis is an indispensable activity in chemical plant design. A wealth of methods, procedures, algorithms and approaches have been proposed (Mizsey and Fonyo, 1990; Douglas et al., 1993; Qian and Lien, 1995; Douglas, 1995; Siirola, 1996; among others). Some of these have been implemented in computer codes for developing separation processes (Wahnschafft et al., 1991; Brunet and Liu, 1993; among others). Many methods are rule-driven; heuristics and facts are used to help generate flowsheet alternatives. The work of Barnicki and Fair (1990, 1992), as well as Barnicki and Siirola (1997) which contains a comprehensive set of heuristics for separating liquid and gas/vapor mixtures, typifies this approach. A considerably different method was suggested by Jaksland et al. (1995) and Gani and Constantinou (1996). For a multicomponent mixture, pure component properties such as kinetic diameter, van der Waals volume, polarizability, melting point, and boiling point are used to determine where a split should occur for each type of separation technique including distillation, crystallization, absorption, extraction, adsorption, membranes, and others.

While these existing methods provide excellent alternatives for some separation sequences, none considers explicitly and generally the extent to which *process boundaries* limit recovery (O'Young et al., 1997). This is important because a seemingly feasible separation can be blocked. For example, a heuristic states that crystallization is very feasible if the melting point ratio for a binary pair is larger than 1.2 (Jaksland et al., 1995). However, such a separation may not be possible because of the presence of a *thermodynamic process boundary* caused by eutectics or compound formation. An analogous problem occurs in distillation where a separation can be limited by a process boundary caused by azeotropes. Crystallization boundaries have been examined by Dye and Ng (1995b) and Berry and Ng (1997a), while distillation boundaries have been examined by Ahmad and Barton (1996), Safrit and Westerberg (1997), and Ahmad et al. (1998), among others. A similar limitation can be imposed by an *equipment process boundary.* For example, the permeability and design of a membrane unit can limit the feasible separation. For a given feed, feasible separations can be represented within the composition space using an equipment process boundary beyond which the permeate and retentate compositions cannot be reached (Pressly and Ng, 1998). The objective of this study is to formulate a framework to consider these process boundaries in designing a separation system. Special emphasis is placed on crystallization, distillation and membrane processes, and on systems with four or more components for which graphical representation of process boundaries is difficult. This work is not intended to be a stand-alone method; rather, it serves as one of the tools in the repertoire of heuristics, algorithms, and so on for separation systems synthesis.

Correspondence concerning this article should be addressed to K. M. Ng.

Composition Space and Process Boundaries

Separations synthesis of an n-component mixture in a continuous process can be viewed in n-dimensional composition space as follows. A stream of composition x^F is transformed using appropriate separation techniques into p product streams, each of which is represented by a composition vector x^P. An N-dimensional space is needed if $(N-n)$ separating agents are used to separate the n-component mixture.

Process boundaries are functions or sets of functions of the mole fractions which define the composition space. For example, solubility surfaces in solid-liquid equilibrium (SLE), immiscibility envelopes in liquid-liquid equilibrium (LLE), and distillation boundaries in vapor-liquid equilibrium (VLE) composition spaces can be described by mathematical functions. In many cases, such boundaries are approximately linear as in many SLE boundaries. Nonlinear boundaries can be approximated using sets of linear boundaries. Therefore, we outline below only a linear representation method for process boundaries.

For an N component system, an $(N-1)$ dimensional composition space in mole fractions is needed. The general equation of an $(N-2)$ dimensional hyperplane is

$$a_1 x_1 + a_2 x_2 + a_3 x_3 + \dots + a_{N-1} x_{N-1} + b = 0 \qquad (1)$$

where a_i's and b are constant parameters. Such a hyperplane of dimension $N-2$ is referred to as a *boundary* which can be defined by using $N-1$ points to determine the $N-1$ independent parameters. These boundaries partition the composition space into *regions*. If the dimension of a hyperplane, $M-1$, is less than $N-2$, the hyperplane is described by the following set of equations

$$\begin{aligned} x_1 &= a_{11} t_1 + a_{12} t_2 + \dots + a_{1,M-1} t_{M-1} + b_1 \\ x_2 &= a_{21} t_1 + a_{22} t_2 + \dots + a_{2,M-1} t_{M-1} + b_2 \\ &\dots \\ x_{N-1} &= a_{N-1,1} t_1 + a_{N-1,2} t_2 + \dots + a_{N-1,M-1} t_{M-1} + b_{N-1} \end{aligned} \qquad (2)$$

where the a_{ij}'s and b_i's are constant parameters and the t_i's are variable parameters. In this case, M points are required to determine the $M(N-1)$ parameters. For each point, a selection of values for the t_i's is necessary. A convenient assignment is to set t_i to be zero for one of the M points; this allows the determination of $b_1, \dots, b_{N-1}$. For the other $M-1$ points, each $M-1$ t_i is set in turn to be one and the rest zero; this allows the determination of $(a_{11}, a_{21}, \dots, a_{N-1,1})$, $\dots$, $(a_{1,M-1}, a_{2,M-1}, \dots, a_{N-1,M-1})$. Also note that Eq. 1 can be recovered from Eq. 2 if M equals $N-1$.

For a line in $N-1$ dimensions, the parametric equations can be obtained by setting M equal to two in Eq. 2

$$\begin{aligned} x_1 &= a_1 t + b_1 \\ x_2 &= a_2 t + b_2 \\ &\dots \\ x_{N-1} &= a_{N-1} t + b_{N-1} \end{aligned} \qquad (3)$$

The parameters can be determined using two points x^1 and x^2. The point of intersection x^3 of a line with a boundary or a hyperplane of dimension less than $N-2$ can be found by substituting the vector x from Eq. 3 into Eq. 1 or Eq. 2, respectively.

Let us represent an $(N-2)$ dimensional hyperplanes in Eq. 1 as $g_1(x)$, $g_2(x)$, and so on. The points between two boundaries can be described by using inequalities. For example, for a point x' to lie in a region between g_1 and g_2 where $g_1 \leq g_2$, we have

$$g_1(x') < 0, \qquad (4a)$$

and

$$g_2(x') > 0 \qquad (4b)$$

Boundaries Formed by Eutectics and Azeotropes

Earlier studies on thermodynamic process boundaries focus primarily on ternary and quaternary mixtures. The synthesis of crystallization processes to bypass eutectic boundaries was discussed by Cisternas and Rudd (1993), Dye and Ng (1995a), and Berry and Ng (1996). The use of residue curves and distillation lines for designing systems with distillation boundaries was discussed by Fien and Liu (1994), Malone and Doherty (1995), and Widagdo and Seider (1996). Synthesis of hybrid crystallization-distillation processes involving both eutectic and distillation boundaries was considered by Berry and Ng (1997b).

The developments for systems with more than four components are more recent. Rooks (1997) presented a systematic method for determining distillation regions based on the reachability concept, while Berry (1997) focused on crystallization regions using a similar approach. Ahmad and Barton (1996) and Ahmad et al. (1998) discussed how to identify the regions and product sequences for azeotropic batch distillation. Safrit and Westerberg (1997) proposed an algorithm with which both continuous and batch distillation regions can be found; they also presented a review of the existing literature.

In this study, we use a region finding method related to that of Rooks (1997) and Berry (1997) for describing the geometrical varieties in an $N-1$ dimensional space (Table 1). It

Table 1. Procedure for Determining the Crystallization and Distillation Boundaries in a Composition Space

(1) Determine and classify the fixed points into saddles, stable nodes, and unstable nodes.
(2) Link the fixed points with directed connections.
(3) Determine all of the paths starting at an unstable node, pro ceeding in the direction of the connections and ending on a stable node.
(4) Group the paths into regions which start at the same unstable node and terminate on the same stable node.
(5) Identify all of the points shared by any two regions. These are the points which describe the boundaries.
(6) Identify hyperplanes with a dimension one less than that of the boundary, if necessary.
(7) Repeat Step 6 by further reducing the dimension until the hyperplane is actually a point, if necessary.
(8) Solve for the parameters needed to describe the boundaries as linear hyperplanes using Eq. 1.
(9) Check for and remove false regions, if necessary.
(10) Check for and remove nonconvex boundaries, if necessary.

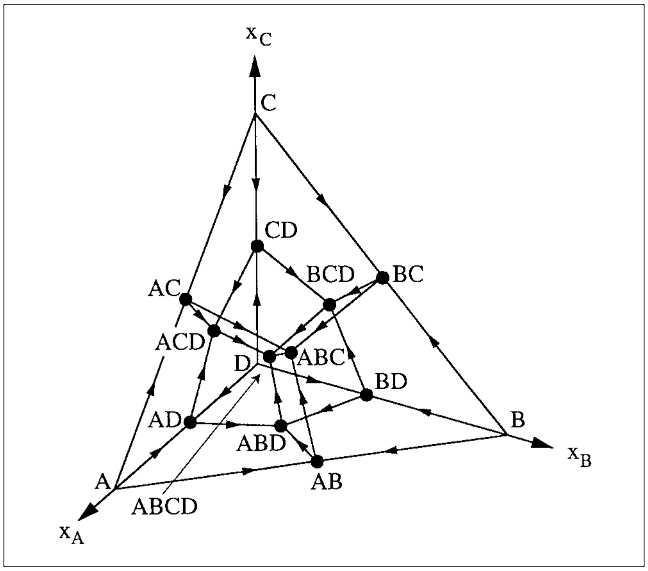

Figure 1a. Solid-liquid equilibrium composition space for a simple eutectic system.

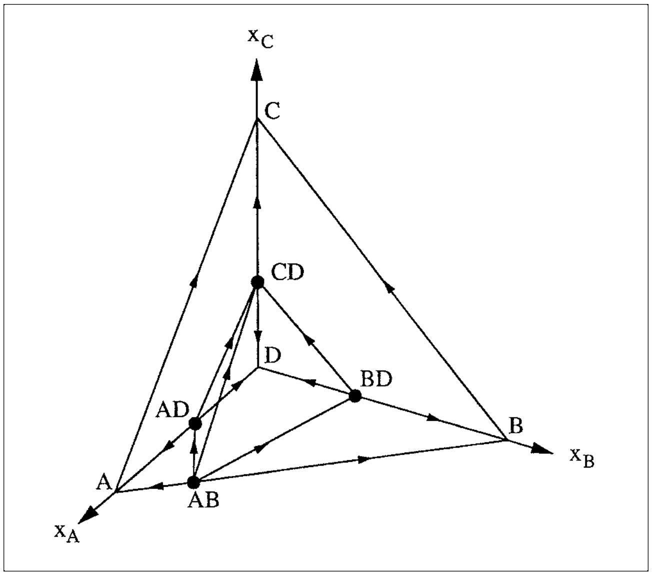

Figure 1b. Vapor-liquid equilibrium composition space for a system with four binary eutectics.

is relatively simple to implement and has worked for the cases considered. However, no general proof is available at this time. To fix ideas, two quaternary mixtures—a solid-liquid equilibrium (SLE) composition space with four eutectic boundaries (Figure 1a) and a vapor-liquid equilibrium (VLE) composition space with two distillation boundaries (Figure 1b)—are used to illustrate the procedure. In Step 1, the fixed points in the composition space are determined and classified into saddles, stable and unstable nodes. The classification for Figure 1a is as follows: pure components A, B, C, and D are unstable nodes; quaternary eutectic ABCD is a stable node; all binary and ternary eutectics are saddles. In Step 2, the fixed points are connected with each *connection* between two fixed points pointing in the direction of decreasing temperature. In Step 3, starting with an unstable node and ending with a stable node, a *path* is generated by following the directed connections. Figure 1a contains 24 paths, some of which are: A-AB-ABC-ABCD, A-AB-ABD-ABCD, A-AC-ABC-ABCD, A-AC-ACD-ABCD, A-AD-ABD-ABCD, A-AD-ACD-ABCD, B-AB-ABC-ABCD, B-AB-ABD-ABCD, and so on. In Step 4, the paths are grouped into regions. Within each region, the paths start at the same unstable node and terminate on the same stable node. The fixed points made up of these paths are the points of this region. For example, the region for component A is made up of the first six of the eight paths listed above; the points for region A are A, AB, AC, AD, ABC, ABD, ACD, ABCD. In Step 5, a boundary shared by two contiguous regions is identified by matching the points belonging to these two regions. For example, the points of the boundary shared by regions A and B are AB, ABC, ABD, and ABCD. Note that in general there are ${}_N C_2$ boundaries for simple eutectic systems. In this four component example, we have the six boundaries each between one of the following sets of regions: A and B, A and C, A and D, B and C, B and D, and C and D.

In Step 6, the hyperplanes with a dimension one less than that of the boundary (that is, $N-2$) are identified by matching the points of each pair of boundaries. The ternary eutectic trough ABD-ABCD along which components A, B and D coprecipitate is such an example. Examples of separation schemes where the eutectic troughs play a key role can be found in Berry and Ng (1996). In Step 7, we identify the hyperplanes of successively lower dimensions by matching the

Table 2. The Fixed Points, Boundaries and Regions for the SLE Composition Space in Figure 1a

Boundary Points	
Eutectic	*Composition*
ABCD	(0.250, 0.250, 0.250, 0.250)
ABC	(0.333, 0.333, 0.333, 0.000)
ABD	(0.333, 0.333, 0.000, 0.333)
ACD	(0.333, 0.000, 0.333, 0.333)
BCD	(0.000, 0.333, 0.333, 0.333)
AB	(0.500, 0.500, 0.000, 0.000)
AC	(0.500, 0.000, 0.500, 0.000)
AD	(0.500, 0.000, 0.000, 0.500)
BC	(0.000, 0.500, 0.500, 0.000)
BD	(0.000, 0.500, 0.000, 0.500)
CD	(0.000, 0.000, 0.500, 0.500)
Equations for Boundaries	
Equation	*Boundary Points*
$x_A - x_B = 0$	AB, ABC, ABD, ABCD
$x_A - x_C = 0$	AC, ABC, ACD, ABCD
$2x_A + x_B + x_C - 1 = 0$	AD, ABD, ACD, ABCD
$x_B - x_C = 0$	BC, ABC, BCD, ABCD
$x_A + 2x_B + x_C - 1 = 0$	BD, BCD, ABD, ABCD
$x_A + x_B + 2x_C - 1 = 0$	CD, ACD, BCD, ABCD
Equations for Regions	
Region A:	*Region B:*
$x_A - x_B > 0$	$x_A - x_B < 0$
$x_A - x_C > 0$	$x_B - x_C > 0$
$2x_A + x_B + x_C - 1 > 0$	$x_A + 2x_B + x_C - 1 > 0$
Region C:	*Region D:*
$x_A - x_C < 0$	$2x_A + x_B + x_C - 1 < 0$
$x_B - x_C < 0$	$x_A + 2x_B + x_C - 1 < 0$
$x_A + x_B + 2x_C - 1 > 0$	$x_A + x_B + 2x_C - 1 < 0$

Table 3. Connectivity Matrix for the Simple Eutectic Polythermal Solid-Liquid Equilibrium Phase Behavior

	A	B	C	D	AB	AC	AD	BC	BD	CD	ABC	ABD	ACD	BCD	ABCD
A	1	0	0	0	1	1	1	0	0	0	0	0	0	0	0
B	0	1	0	0	1	0	0	1	1	0	0	0	0	0	0
C	0	0	1	0	0	1	0	1	0	1	0	0	0	0	0
D	0	0	0	1	0	0	1	0	1	1	0	0	0	0	0
AB	1	1	0	0	1	0	0	0	0	0	1	1	0	0	0
AC	1	0	1	0	0	1	0	0	0	0	1	0	1	0	0
AD	1	0	0	1	0	0	1	0	0	0	0	1	1	0	0
BC	0	1	1	0	0	0	0	1	0	0	1	0	0	1	0
BD	0	1	0	1	0	0	0	0	1	0	0	1	0	1	0
CD	0	0	1	1	0	0	0	0	0	1	0	0	1	1	0
ABC	0	0	0	0	1	1	0	1	0	0	1	0	0	0	1
ABD	0	0	0	0	1	0	1	0	1	0	0	1	0	0	1
ACD	0	0	0	0	0	1	1	0	0	1	0	0	1	0	1
BCD	0	0	0	0	0	0	0	1	1	1	0	0	0	1	1
ABCD	0	0	0	0	0	0	0	0	0	0	1	1	1	1	1

points of hyperplanes with a dimension one higher. In this example, an even lower dimensional variety is the quaternary eutectic ABCD. In Step 8, the parameters in Eq. 1 for describing the boundaries as linear hyperplanes are determined. The results of this step for the example are displayed in Table 2.

Description of high dimensional systems can be facilitated by using the *connectivity matrix*. Each element represents a pair of points and is described by the following

$$A_{ij} = 1, \text{ if } i \text{ is connected to } j \tag{5}$$

and

$$A_{ij} = 0, \text{ if } i \text{ is not connected to } j \tag{6}$$

Table 3 is the connectivity matrix for the simple eutectic polythermal solid-liquid equilibrium composition space displayed in Figure 1a. Another useful representation is the *adjacency matrix*, which is analogous to the connectivity matrix, but incorporates the directionality of the connections (Table 4). If the point in row *i* is connected to and directed toward the point in row *j*, the element *ij* has a value of one. For any other case, the element *ij* would be zero. Even if Figure 1a is not available, the 24 paths can be readily generated with the adjacency matrix. Beginning with row A in Table 4, it can be seen that A is connected to AB. From row AB, we see that AB is connected to ABC. Row ABC shows that ABC is connected to ABCD. Thus, the A-AB-ABC-ABCD path has been identified. The adjacency matrix is usually used in combination with the *reachability matrix*, which can be obtained from the adjacency matrix. Starting at a point in row *i* of this matrix, if the point in column *j* can be reached by moving along the directed connections, the element *ij* is unity. In all other cases, the element would be zero. The reachability matrix for the SLE example is displayed in Table 5.

Figure 1a is a polythermal diagram within which each point can have a different temperature. It is suitable for describing cooling crystallization, as well as extractive crystallization schemes (Dye and Ng, 1995a). For isothermal evaporative crystallization, isothermal diagrams such as those presented in Dye and Ng (1995b) should be used for representing the composition space.

The same procedure is applicable for the vapor-liquid equilibrium composition space (Figure 1b) with four binary azeotropes: AB, AD, BD, and CD. The fixed points, boundaries, and regions are displayed in Table 6. A few remarks need to be made. In Step 2, opposite to that of crystallization, the connection between two fixed points should point in the direction of increasing temperature. As can be seen in Figure 1b, Step 5 identifies a boundary AB-AD-BD-CD which is made up of more than one linear plane. When this occurs,

Table 4. Adjacency Matrix for the Simple Eutectic Polythermal Solid-Liquid Equilibrium Phase Behavior

	A	B	C	D	AB	AC	AD	BC	BD	CD	ABC	ABD	ACD	BCD	ABCD
A	0	0	0	0	1	1	1	0	0	0	0	0	0	0	0
B	0	0	0	0	1	0	0	1	1	0	0	0	0	0	0
C	0	0	0	0	0	1	0	1	0	1	0	0	0	0	0
D	0	0	0	0	0	0	1	0	1	1	0	0	0	0	0
AB	0	0	0	0	0	0	0	0	0	0	1	1	0	0	0
AC	0	0	0	0	0	0	0	0	0	0	1	0	1	0	0
AD	0	0	0	0	0	0	0	0	0	0	0	1	1	0	0
BC	0	0	0	0	0	0	0	0	0	0	1	0	0	1	0
BD	0	0	0	0	0	0	0	0	0	0	0	1	0	1	0
CD	0	0	0	0	0	0	0	0	0	0	0	0	1	1	0
ABC	0	0	0	0	0	0	0	0	0	0	0	0	0	0	1
ABD	0	0	0	0	0	0	0	0	0	0	0	0	0	0	1
ACD	0	0	0	0	0	0	0	0	0	0	0	0	0	0	1
BCD	0	0	0	0	0	0	0	0	0	0	0	0	0	0	1
ABCD	0	0	0	0	0	0	0	0	0	0	0	0	0	0	0

Table 5. Reachability Matrix for the Simple Eutectic Polythermal Solid-Liquid Equilibrium Phase Behavior

	A	B	C	D	AB	AC	AD	BC	BD	CD	ABC	ABD	ACD	BCD	ABCD
A	1	0	0	0	1	1	1	0	0	0	1	1	1	0	1
B	0	1	0	0	1	0	0	1	1	0	1	1	0	1	1
C	0	0	1	0	0	1	0	1	0	1	1	0	1	1	1
D	0	0	0	1	0	0	1	0	1	1	0	1	1	1	1
AB	0	0	0	0	1	0	0	0	0	0	1	1	0	0	1
AC	0	0	0	0	0	1	0	0	0	0	1	0	1	0	1
AD	0	0	0	0	0	0	1	0	0	0	0	1	1	0	1
BC	0	0	0	0	0	0	0	1	0	0	1	0	0	1	1
BD	0	0	0	0	0	0	0	0	1	0	0	1	0	1	1
CD	0	0	0	0	0	0	0	0	0	1	0	0	1	1	1
ABC	0	0	0	0	0	0	0	0	0	0	1	0	0	0	1
ABD	0	0	0	0	0	0	0	0	0	0	0	1	0	0	1
ACD	0	0	0	0	0	0	0	0	0	0	0	0	1	0	1
BCD	0	0	0	0	0	0	0	0	0	0	0	0	0	1	1
ABCD	0	0	0	0	0	0	0	0	0	0	0	0	0	0	1

the set of points for a boundary is further divided so that a set of points is obtained for each individual linear boundary in that composite boundary.

As discussed in Safrit and Westerberg (1997), for some phase behavior, it is possible to generate a path such that the starting unstable node is in a different region than the terminating stable node. These paths can lead to sets of fixed points which are false regions. It is therefore necessary to apply the following test once all of the candidate regions have been identified. A boundary can only be shared by two true regions. If a boundary is shared by three or more candidate regions, the false regions have to be eliminated by trial and error (Step 9).

Once all of the boundaries have been identified for a region, the region should be tested for convexity. The solid-liquid equilibrium system contains only convex regions. If the region is found to be convex, the inequalities of Eqs. 4a and 4b can be used directly to define the region.

If the region is nonconvex, the nonconvexity can be removed by subdivision (Step 10). One of the two boundaries around which a nonconvexity is found is extended until it intersects another boundary in the region, so that two regions are produced. This process is continued until only convex regions exist. The VLE composition space in Figure 1b contains an example of one convex region (D, AB, AD, BD, CD) and one nonconvex region (A, AB, AD, CD, B, BDC). The convex region is referred to as region 2. The nonconvex region is divided into two parts by extending the plane AB-BD-CD. Two convex regions, regions 1a and 1b, result. These two convex subregions together make up the larger nonconvex region. The resulting inequalities are displayed in Table 6.

Table 6. Fixed Points, Boundaries, and Regions for the VLE Composition Space in Figure 1b

Boundary Points

Azeotrope	*Composition*
AB	(0.800, 0.200, 0.000, 0.000)
AD	(0.400, 0.000, 0.000, 0.600)
BD	(0.000, 0.400, 0.000, 0.600)
CD	(0.000, 0.000, 0.350, 0.650)

Equations for Boundaries

Equation	*Boundary Points*
$0.875x_A + 3.50x_B + 4.00x_C - 1.40 = 0.000$	AB, BD, CD
$0.875x_A - 1.75x_B + 1.00x_C - 0.350 = 0.000$	AB, AD, CD

Equatons for Regions

Region 1a:

$0.875x_A + 3.50x_B + 4.00x_C - 1.40 < 0.000$

$0.875x_A - 1.75x_B + 1.00x_C - 0.350 > 0.000$

Region 1b:

$0.875x_A + 3.50x_B + 4.00x_C - 1.40 > 0.000$

Region 2:

$0.875x_A + 3.50x_B + 4.00x_C - 1.40 < 0.000$

$0.875x_A - 1.75x_B + 1.00x_C - 0.350 < 0.000$

Boundaries Formed by Liquid-Liquid Equilibrium

A liquid-liquid phase split results in boundaries which are typically fairly nonlinear. Often, these boundaries cannot be adequately approximated with a single linear hyperplane. However, several hyperplanes can be used to approximate the boundary. For example, in a quaternary LLE composition space, linear planes each defined by three points can be fit onto the LLE envelope. In other words, the surface of the LLE envelope is divided into triangles. The region representing the LLE envelope can then be described with inequalities (Eqs. 4a and 4b).

Boundaries Formed by Solid Phase Separating Agents

For separation systems in which a solid separating agent such as an adsorbent or a membrane is used, the separating agent does not form an additional component in the system because it remains in the equipment unit. However, the separation is limited by the interaction of the separating agent and the mixture to be separated, instead of just the thermodynamics of the mixture itself. It is highly desirable to identify the equipment boundary within which the product composition can be reached. This is illustrated with membrane separation in terms of three vectors in a composition space: the *permeate vector* from the feed to the permeate S_P, the *retentate vector* from the feed to the retentate S_R, and the *total separation vector* from the retentate to the permeate S_T.

The retentate vector is related to the permeate vector through the membrane cut as follows

$$S_R = -S_P\theta/(1-\theta) \tag{7}$$

The total separation vector shares the direction of the permeate vector, and can be calculated as follows

$$S_T = S_P/(1-\theta) \tag{8}$$

Here, the membrane cut is the ratio of molar flow rate of permeate P to that of the feed F

$$\theta = \frac{P}{F} \tag{9}$$

In turn, the permeate vector for a given feed can be determined with the separation factor, a general definition of which is

$$\alpha_{ij} = \frac{x_i^P x_j^F}{x_i^F x_j^P} \tag{10}$$

For an N component system, the use of $N-1$ separation factors leads to the permeate composition

$$x_i^P = \frac{\alpha_{iN} x_i^F}{\Sigma \alpha_{iN} x_i^F} \tag{11}$$

Thus, the separation factors provide a direction for the separation and a distance between the feed and permeate composition, while the membrane cut equation (Eq. 7) allows the distance of the retentate composition from the feed along the material balance line to be determined. It should be noted that this procedure can be similarly repeated to solve for the feed compositions if the permeate compositions are specified.

Example with a ternary mixture

Applying Eq. 11 results in the following two equations for ternary systems

$$x_1^P = \frac{\alpha_{13} x_1^F}{\alpha_{13} x_1^F + \alpha_{23} x_2^F + x_3^F} \tag{12}$$

$$x_2^P = \frac{\alpha_{23} x_2^F}{\alpha_{13} x_1^F + \alpha_{23} x_2^F + x_3^F} \tag{13}$$

Rather than evaluating specific membranes one at a time, it is desirable to determine the feasible separations for a given feed and a given set of membrane characteristics. This can be achieved by setting a maximum separation factor to determine the process boundary on the permeate. There are six separation factors which could be set to this maximum value: α_{12}, α_{23}, α_{13}, and their inverses α_{21}, α_{32}, α_{31}. In order to get the limitation of this maximum separation factor, one separation factor is set to the maximum. The other separation factors are varied with the constraint that no separation factor becomes greater than the maximum. Then another one of the six separation factors is held at the maximum, while the other separation factors are varied. Once each of the separation factors has been held at the maximum, the complete boundary of the permeate compositions is generated. The results of such calculations for a feed of composition of (0.333, 0.333, 0.334) and maximum separation factors of 20 and 5 are displayed in Figure 2a. Note that with a high separation factor of 20 the permeate composition can reach almost the entire composition space. In Figure 2b, the effect of the initial feed concentration on the possible permeate compositions are displayed. In this figure, the feed composition is (0.1, 0.1, 0.8), while the maximum separation factors are kept at 20 and 5. As can be seen, the initial feed can have a large impact on the magnitude of the separation possible.

There are situations in which the permeate composition is specified. For a membrane with a given set of characteristics, the problem is to determine the feed composition which yields such permeate purity. The feed compositions may be determined from the permeate compositions for a ternary system as follows

$$x_1^F = \frac{x_1^P/\alpha_{13}}{x_1^P/\alpha_{13} + x_2^P/\alpha_{23} + x_3^P} \tag{14}$$

$$x_2^F = \frac{x_2^P/\alpha_{23}}{x_1^P/\alpha_{13} + x_2^P/\alpha_{23} + x_3^P} \tag{15}$$

It is assumed in Figure 2c that the permeate stream must contain at least 0.995 mol fraction of component A. It shows that the feed must lie above the respective horizontal line for separation factors of 50 and then 100 for α_{AB} and α_{AC}.

Design Procedure

With the process boundaries and feasible products identified, generation of flowsheet alternatives begin. An outline of the design procedure is displayed in Table 7. In this procedure, the feed composition and flow rate, as well as the desired products and product compositions, are assumed to be specified (Steps 1 and 2). Then, the separation sequence is determined in a step-by-step manner by moving the feed composition through the composition space towards the product compositions. In Step 3, beginning with the feed, either the heuristic-based methods suggested by Barnicki and Fair (1990, 1992) and others, or the physical/chemical properties method by Jaksland et al. (1995) can be used to identify feasible and infeasible separation techniques. In Step 4, the boundaries, regions, and feasible products for the units which are deemed applicable are determined using the procedure in Table 1. In Step 5, the parameters describing the boundaries (Eq. 1), are determined. In Step 6, we substitute the selected feed composition (x^F) and one product composition (x^{P1}) into Eq. 3 to determine the material balance line. Then, the intersection point of this material balance line with

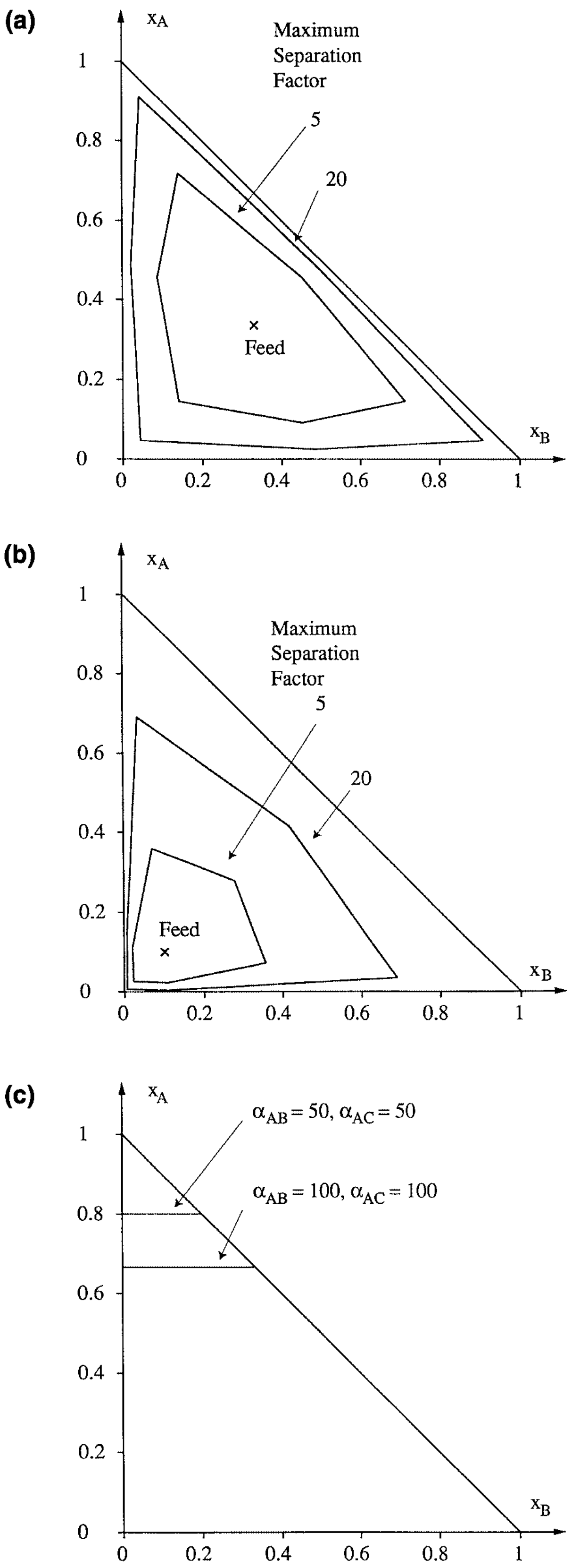

Figure 2. Equipment boundaries.

(a) On the membrane permeate composition for an equimolar feed; (b) on the membrane permeate composition for a feed of (0.1, 0.1, 0.8); (c) on the membrane feed composition for a permeate purity of 0.995 mole fraction A.

Table 7. Design Procedure Accounting for Boundaries in Separations

(1) Specify the flow rate and composition of the overall feed to the separation system.
(2) Decide on the flow rate and composition of each product stream.
(3) Beginning with the feed, use heuristics or physical/chemical properties to identify feasible units and to exclude infeasible units for the current separation step in the flowsheet.
(4) For the current step, determine the relevant thermodynamic and equipment boundaries, regions and the corresponding feasible products.
(5) Determine the linear mathematical form of the thermodynamic and equipment boundaries for the separation technique under consideration, if applicable.
(6) For a proposed separation, determine the intersection point between the material balance line (Eq. 3) and a boundary (Eq. 1).
(7) Repeat Steps 3 to 6 for the current mixture(s) to be separated. Alternative separation techniques at a separation step constitute process alternatives.
(8) After completing the flowsheet, send recycle stream(s) back to the process. Select a recycle destination with a composition comparable to that of the recycle stream. If such destinations do not exist, direct the recycle stream to a destination in such a way that the feed location to each unit remains in the same region of the composition space. Iterate if necessary.

the boundaries in this region is determined by solving Eqs. 1 and 3.

Several candidate products (intersection points) may be generated from these solutions. Each point is tested using the region inequalities. The real intersection point is the largest value of t, which still satisfies all of the inequalities except for the boundary on which the intersection occurs. At this boundary, the inequality becomes an equality of zero. In the event that a nonconvex region has been identified and fixed by subdivision, care should be taken to test all of the parts of the region.

In Step 7, Steps 3 and 6 are repeated for the current location(s) in the composition space until the target product compositions are reached. After removing the desirable products, byproducts, and wastes (Douglas, 1995), the recycle structure needs to be considered in order to synthesize the entire flowsheet. At this point of the design, certain streams for which a destination has not yet been designated arise along the main processing train. In general, these streams have a relatively low flow rate, but contain many of the desirable products. Instead of processing such a stream further using a new separation unit, it is combined with a feed stream of another separations unit. The composition of this combined feed should stay in the same region as the original feed so that the sequence of separations remains the same. Therefore, the recycle stream should be recycled back into the process to the stream with the nearest composition (Step 8). The final flow rate and composition values are obtained by iteration. It may happen that the original feed stream is mixed with a recycle stream to form a new feed stream which is located in another region of the composition space than that of the original feed stream. This will lead to new process alternatives. Also, some of these undesignated streams may contain a significant fraction of wastes and may be purged. Such a decision is case specific and has to be considered in conjunction with waste treatment costs.

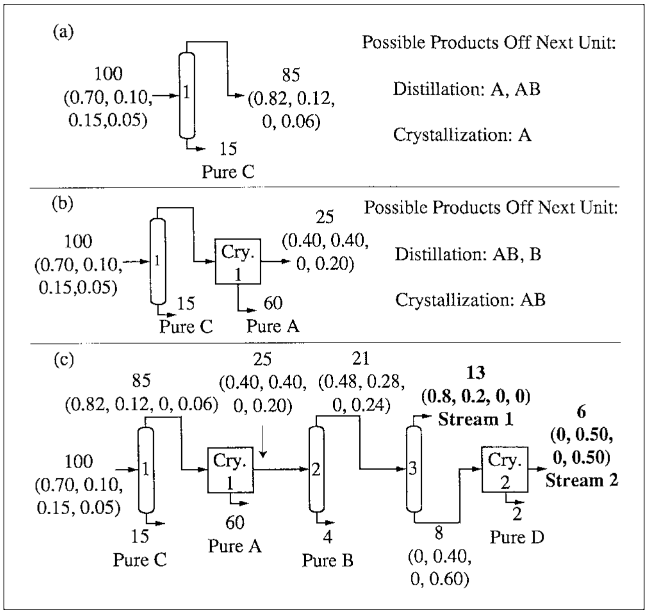

Figure 3. Steps in the flowsheet formation for Example 1.

Implementation

Our calculational procedure is implemented using a spreadsheet. After all of the boundaries and the inequalities for the regions have been determined, the region for the feed is located using the inequalities for each of the separation techniques selected based on heuristics. One separation unit is then added as a block to the spreadsheet and, in anticipation of possible recycle streams, three feeds are used for each separation unit. At this point, only one feed is connected (that is, the other feed flow rates are set to zero). One product composition is chosen from the feasible products for the region in which the unit is operating in and entered into the spreadsheet. The intersection of the material balance line with a boundary has the following general result for the parameter t

$$t = \frac{a_1 x_1^{P1} + a_2 x_2^{P1} + \ldots + a_{N-1} x_{N-1}^{P1} + b}{a_1\left(x_1^{P1} - x_1^F\right) + a_2\left(x_2^{P1} - x_2^F\right) + \ldots + a_{N-1}\left(x_{N-1}^{P1} - x_{N-1}^F\right)} \tag{16}$$

where x^{P1} and x^F are the first product and feed compositions, respectively. The largest value of t which is still in the region under consideration is the location of the other product on the material balance line. The composition of this product is calculated using Eq. 3.

This process of adding units is continued until the separations objective has been met. The recycle structure is determined, as discussed earlier, by matching similar compositions. A macro is programmed to put the compositions and flow rates of the recycle streams in as feed streams to the appropriate units. Using this macro, the spreadsheet calculations are iterated until the stream variables converge. At this point, the overall balances and the balances around each unit will be satisfied. It is our experience that all feasible flowsheets will converge. In some cases, a recycle stream may be used to move the location of the feed to a separation unit to a different region than the region which contains the original feed. The location of the combined feed must be assumed for the initial decision.

Examples

Example 1: A distillation-crystallization hybrid for a quaternary mixture

The first example uses the quaternary system discussed earlier with the SLE and VLE phase diagrams in Figures 1a and 1b, respectively. The feed is set at the following flow rate and composition: 100 lb mol/h and (0.70, 0.10, 0.15, 0.05), which represents the mole fractions of A, B, C, and D, respectively. The separations objective is to recovery each component in pure form. The process synthesis procedure described below is illustrated in Figure 3.

This feed is in region 1 for distillation and region A for crystallization. Pure A can be a product with crystallization. For distillation, pure C or the AB azeotrope can be products. Distillation is chosen for the first unit. The material balance line for this separation intersects the ABD face, the base of the tetrahedron (Figure 1b). The product from this interaction has a flow rate and composition of 85 lb mol/h and (0.82, 0.12, 0, 0.06), respectively (Figure 3a). This and other flow rates below have been rounded off.

This stream can produce AB azeotrope (overhead) and pure A (bottoms) with distillation and pure A with crystallization. Using crystallization produces pure A at a flow rate of 60 lb mol/h and a mother liquor at a flow rate and composition of 25 lb mol/h and (0.40, 0.40, 0, 0.20), respectively (Figure 3b). The possible products from this stream are as follows: distillation-AB azeotrope and pure B; crystallization-AB eutectic.

By continuing this procedure, a flowsheet is obtained which produces all the components in pure form (Figure 3c). There are two streams displayed in bold for which destinations have not yet been designated that need to be recycled: Stream 1, 13 lb mol/h, (0.80, 0.20, 0, 0); Stream 2, 7 lb mol/h, (0, 0.50, 0, 0.50). The first preference is to recycle these streams to a stream with a similar composition. By examining the compositions of the other process streams, the feed stream to the first crystallization unit is found to be at a composition similar to Stream 1. However, there is not a process stream which is similar in composition to Stream 2 except for the feed to the last crystallization unit. This is the feed to the unit from which Stream 2 is produced and is obviously not a feasible destination for the recycle. The second preference is to recycle Stream 2 in such a way that it does not change the feed location from one region to another for any of the upstream units. It is found that the overall feed and the feed to the second distillation column are in the same distillation region as Stream 2. The first column removes component C, while Stream 2 is completely depleted of component C. Thus, the overall feed is rejected as a recycle destination. No such problem is encountered with the feed to the second column, which is selected. The flowsheet calculations were iterated until the stream variables converged. The resulting flowsheet

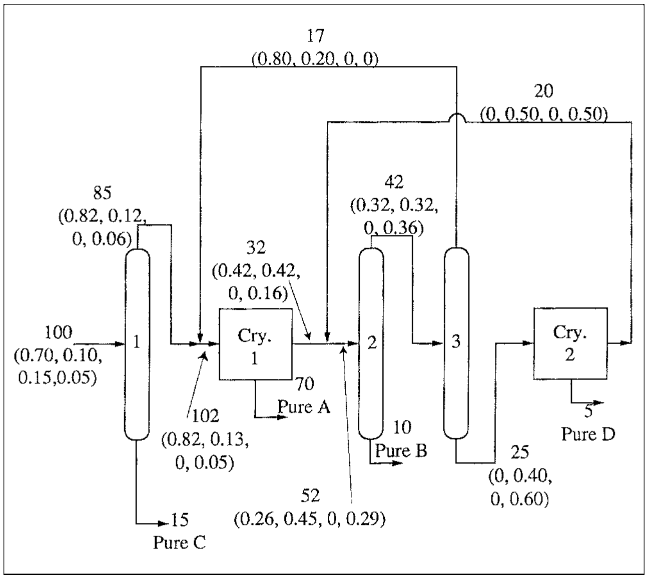

Figure 4. Completed flowsheet for Example 1.

with all of the corrected stream variables is displayed in Figure 4.

Example 2: A distillation-membrane hybrid for a methanol-ethanol-water mixture

There is only one binary minimum boiling azeotrope between ethanol and water in this system (Figure 5). A distillation boundary extends from the pure methanol (an unstable node) to the azeotrope (a saddle). Water and ethanol are both stable nodes. The design procedure leads to the following flowsheet. An equimolar overall feed is assumed.

The combined feed F_1 is sent to the first column which produces a pure water bottoms (0.995 mol fraction water, 0.004 mol fraction ethanol) and an overhead D_1 near the boundary (0.091 mol fraction water, 0.454 mol fraction ethanol). This column requires 20 stages and has a reflux ratio of 1.2. A membrane which selectively permeates water is then used to create a retentate stream R, which is essentially only methanol and ethanol (0.002 mol fraction water, 0.498 mol fraction ethanol), and a permeate stream P to be recycled back to the first column at a composition of 0.180 mol fraction water and 0.409 mol fraction ethanol. To achieve this separation, this membrane would have to have the following properties: a separation factor of water to methanol of 2.2, a separation factor of water to ethanol of 2.2, and a membrane cut of 0.5. The retentate from the membrane is then sent to the second distillation column to produce a distillate (0.995 mol fraction methanol, 0.005 mol fraction ethanol) and a bottoms product (0.995 mol fraction ethanol, 0.004 mol fraction water). This column was sized to have a reflux ratio of 3.2 and 46 stages.

One conventional alternative to this hybrid would be to remove methanol first as a distillate product, leaving a binary solution of ethanol and water. The ethanol-water solution would then be sent to a preconcentrator column to create a distillate near the ethanol-water azeotrope and a bottoms of pure water. This azeotrope stream could then be separated by an extractive or azeotropic distillation process. Note that if extractive distillation using ethylene glycol as an entrainer is used, this process will contain four distillation columns and will require a separating agent.

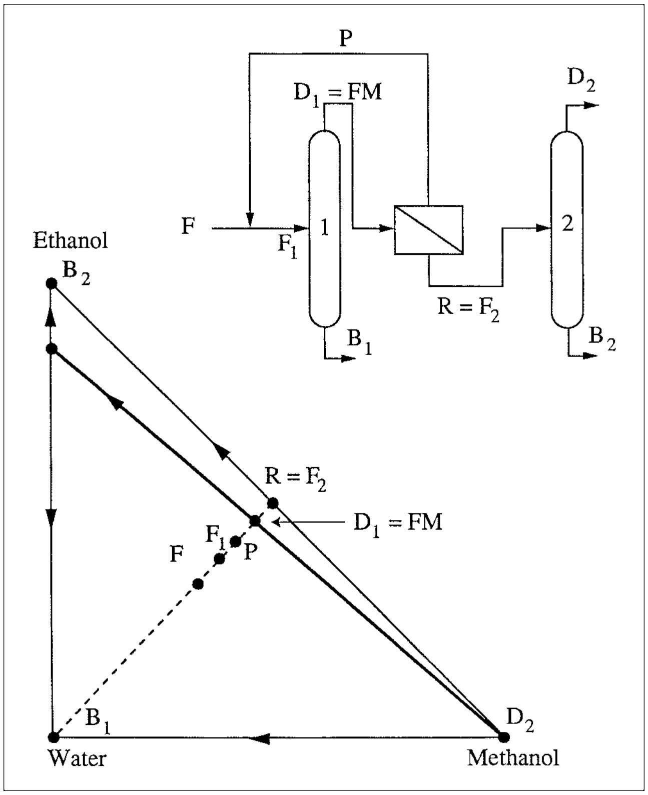

Figure 5. Flowsheet and composition space for separating a methanol-ethanol-water mixture.

Additional examples of flowsheet formulation for ternary distillation-membrane hybrids

The design procedure can be used to generate flowsheet alternatives for systems with similar phase behavior (Figure 6). Note that the following symbols are used: F is overall feed, F_i is the feed to the ith column, D_i is the distillate of the ith column, B_i is the bottoms of the ith column, FM is the membrane feed, P is the permeate, and R is the retentate.

Figure 6a shows a system with a distillation boundary lying near a binary edge (AC), which contains no azeotropes. For this example, the overall feed is near the boundary and the membrane is applied first to bypass the boundary. The retentate and permeate streams are further split into two columns to produce the pure components and the recycle stream D_1.

In the next system, there are three binary azeotropes and one ternary azeotrope (Figure 6b). Each of the three pure components are stable nodes. The distillation boundary is Y shaped. In the first column, one of the components can be recovered (B) and the other product stream (FM) fed to a membrane. The membrane splits the stream into the two other regions. Two distillation columns can then be used to

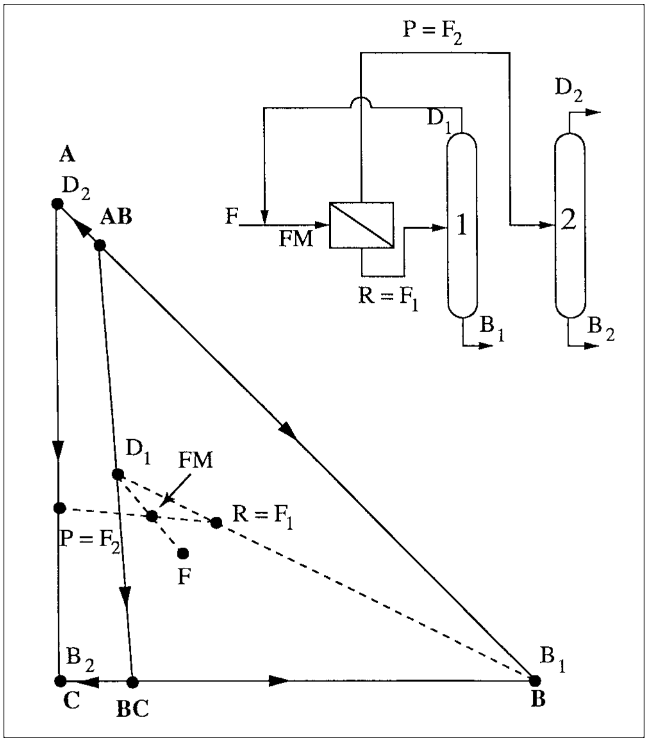

Figure 6a. Flowsheet and accompanying composition space for separating a ternary mixture with one distillation boundary.

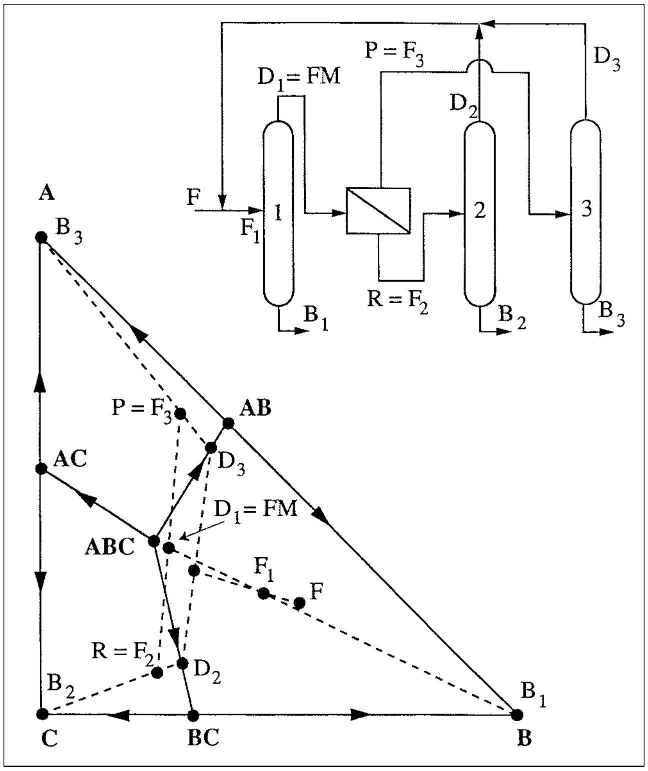

Figure 6b. Flowsheet and accompanying composition space for separating a ternary mixture with a Y-shaped distillation boundary.

produce the remaining two components A and C, while creating two recycle streams.

For the last example system type, there are three alternate configurations (Figures 6c to 6e). This system has a minimum boiling binary azeotrope and a ternary saddle azeotrope. An X shaped distillation boundary is formed. Region A partially overlaps regions B and C; regions B and C do not overlap with each other. As a result, a membrane can be used to move between the parts of regions B and C that overlap with A. For a feed in the A-ABC-B-A region (Figure 6c), component B can be recovered as the bottoms product. The distillate is near the A-ABC boundary and can be fed to a membrane to move into the A-ABC-C-A region. The remaining two pure components are then produced by distillation of the retentate stream. In Figure 6d, the overall feed composition is near the B-ABC boundary, the feed can be first sent to a membrane, which can split the stream into streams in both of the desired regions. The pure components are then recovered by distillation. Figure 6e shows an example with a feed made up of primarily A and C. These most plentiful components are separated first before recovering B in the third distillation column.

Example 3: A quinary system of acetone-methanol-ethanol-2-propanol-water

The separations objective is to recover each of the five components of this equimolar mixture in pure form. This sys-

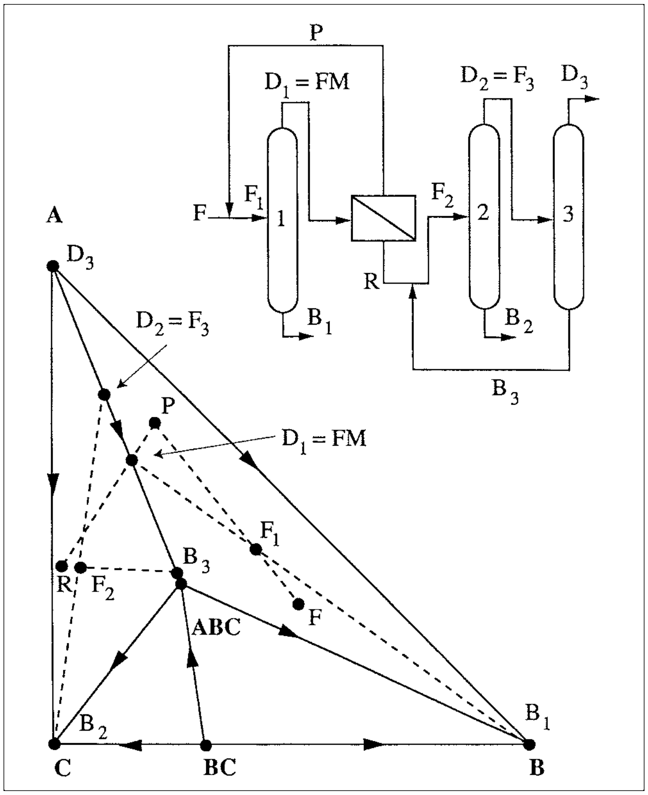

Figure 6c. Flowsheet alternative 1 and accompanying composition space for separating a ternary mixture with an X-shaped distillation boundary.

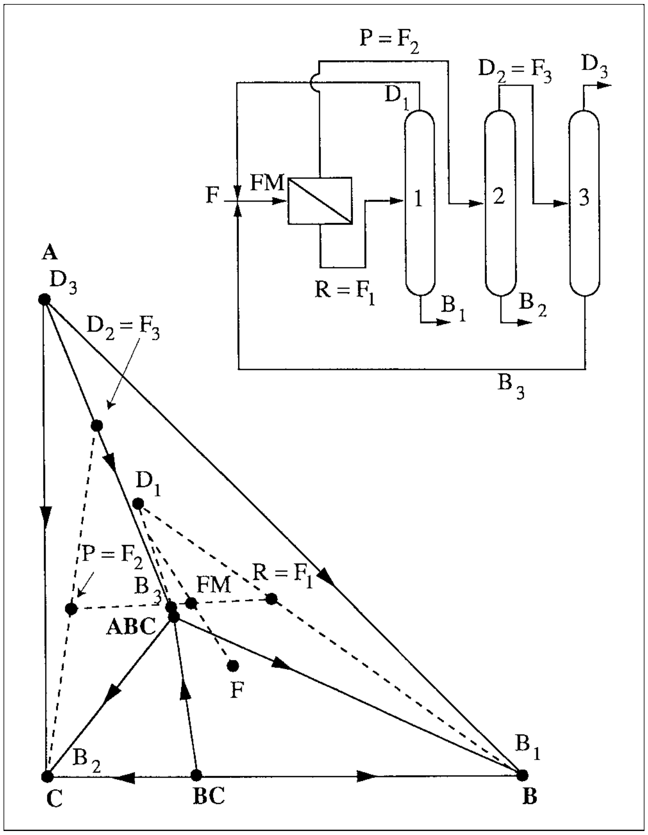

Figure 6d. Flowsheet alternative 2 and accompanying composition space for separating a ternary mixture with an X-shaped distillation boundary.

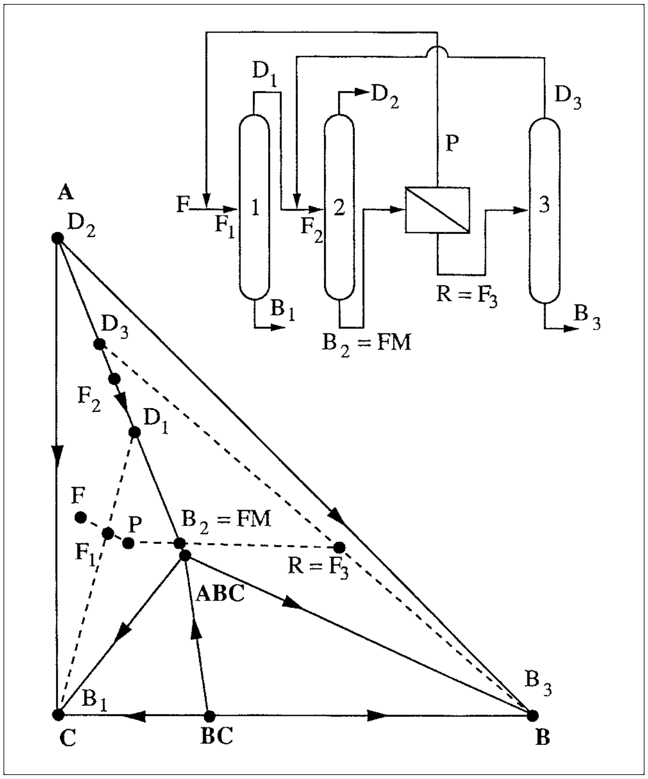

Figure 6e. Flowsheet alternative 3 and accompanying composition space for separating a ternary mixture with an X-shaped distillation boundary.

tem exhibits three binary azeotropes: acetone-methanol, ethanol-water, and 2-propanol-water. Two regions are formed: region 1: acetone, methanol, ethanol, 2-propanol, and the three azeotropes; region 2: acetone, methanol, water, and the three azeotropes. One distillation boundary exists which contains the following points: acetone, methanol, and all three azeotropes. Details of this system are summarized in Table 8. Two of the several possible flowsheets are described below each containing two membranes in the hybrid. One membrane has a separation factor of methanol to acetone of 5. The second membrane has a separation factor of water to each of the organics of 10.

In the first flowsheet (Figure 7), the overall feed is sent to distillation column 1 which produces a water product as a bottoms and a distillate product on the distillation boundary. Molar flow rates and compositions expressed in the mole fraction of acetone, methanol, ethanol, 2-propanol, and water in that order are given for the streams in the figure. The second column takes the distillate from the first column and produces the acetone-methanol azeotrope as a distillate; the bottoms of this column is completely depleted of acetone. The acetone-methanol stream at the azeotropic composition is fed to the first membrane. The membrane boosts the acetone concentration in the retentate. From the retentate, acetone is recovered by the third column. The distillate from the third column is at the same acetone-methanol azeotropic composition and is recycled back to the feed of membrane 1. The membrane permeate concentration is recycled back to the second column.

The bottoms off the second column (depleted in acetone) is sent to the second membrane. This membrane produces a water rich permeate stream, which is recycled back to the first column, and a water lean retentate stream, which is on the opposite side of the distillation boundary than the overall feed. This retentate stream is sent to the fourth distillation column, which produces a pure methanol distillate and a bottoms completely depleted in methanol. The bottoms stream

Table 8. Boiling Points and Classification of the Fixed Points in Example 3

Component	Boiling Point (°C)	Node/Saddle
Acetone	56.1	Saddle
Methanol	64.5	Saddle
Ethanol	78.3	Saddle
2-Propanol	82.2	Stable Node
Water	100.0	Stable Node
Azeotrope	**Boiling Point (°C)**	**Node/Saddle**
Acetone-Methanol	55.3	Unstable Node
Ethanol-Water	78.1	Saddle
2-Propanol-Water	80.4	Saddle

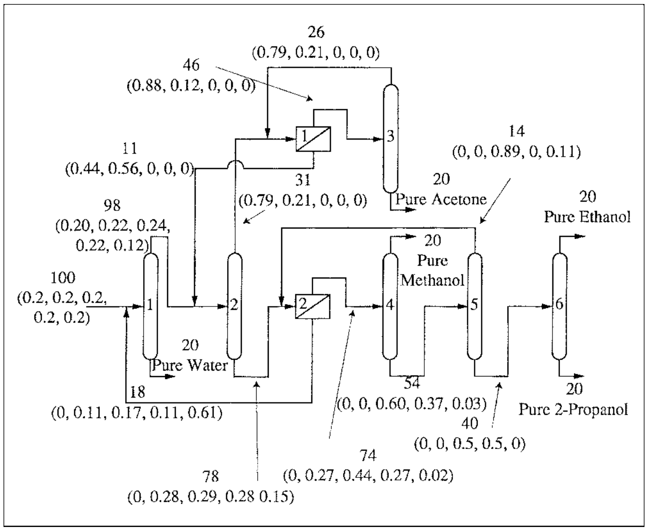

Figure 7. Flowsheet alternative 1 for separating an acetone-methanol-ethanol-2-propanol-water mixture.

is fed to the fifth distillation column, which produces a distillate stream at the ethanol-water azeotropic composition and a bottoms stream completely depleted in water. The distillate stream is recycled back to the second membrane. The bottoms stream is a binary mixture of ethanol and 2-propanol, which is fractionated in the sixth distillation column.

The second flowsheet also is composed of six distillation columns and two membranes (Figure 8). In this flowsheet, the overall feed is sent to the first membrane. This membrane produces a water rich permeate stream on one side of the distillation boundary and a water lean retentate stream on the other side of the boundary. The permeate stream is sent to the first distillation column, in which water is recovered as the bottoms product. The distillate product is on the distillation boundary and is recycled back to the first membrane. The retentate from the first membrane is sent to the second distillation column. This column produces a distillate at the acetone-methanol azeotropic composition and a bottoms completely depleted in acetone. The distillate stream is fed to the second membrane which produces an acetone rich retentate and an acetone lean permeate. The retentate stream is fed to the third column, in which acetone is recovered as a bottoms product. The distillate from the third column (at the acetone-methanol azeotropic composition) is recycled back to the second membrane. The membrane permeate stream is recycled back to the second column.

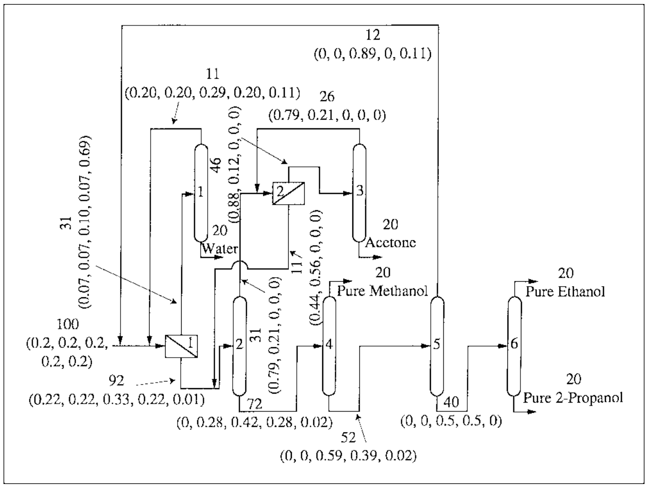

Figure 8. Flowsheet alternative 2 for separating an acetone-methanol-ethanol-2-propanol-water mixture.

The bottoms off the second column is sent to the fourth column in which the remaining methanol is recovered in the distillate. The bottoms of the fourth column (completely depleted in methanol) is sent to the fifth column, which produces a distillate at the ethanol-water azeotropic composition, which is recycled to column 1. The bottoms product of column 5, which contains a binary mixture of ethanol and 2-propanol, is separated in the sixth column.

Example 4: crystallization-decantation hybrid for a quaternary system

In this example, the three component mixture, A, B, C, are completely separated by crystallization. The solid-liquid equilibrium exhibits three binary eutectics and one ternary eutectic: (0, 0.10, 0.90), (0.20, 0, 0.80), (0.91, 0.09, 0), (0.15, 0.07, 0.78), with the elements in each term representing the mole fraction of A, B, and C, respectively. A solvent S is available which is miscible with A and B. The solvent is immiscible with component C over a temperature range which is higher than the temperature range in which the melting surfaces are present. In other words, the immiscibility bubble does not intersect the melting surfaces [see Berry et al. (1997) for such phase diagrams]. The liquid-liquid envelope is approximated using five boundary points which form four connected triangular linear planes (Table 9), that is, a boundary point is shared by all four planes and each pair of planes share two

Table 9. Boundary Points, Boundaries and Regions for the LLE Composition Space in Example 4

Boundary Points

Point	*Composition*
1	(0.000, 0.000, 0.100, 0.900)
2	(0.333, 0.000, 0.333, 0.333)
3	(0.000, 0.333, 0.333, 0.333)
4	(0.236, 0.236, 0.195, 0.333)
5	(0.000, 0.000, 0.900, 0.100)

Equations for Boundaries

Equation	*Boundary Points*
$0.778x_A - 0.329x_B - 1.11x_C + 0.111 = 0$	1, 2, 4
$-0.328x_A + 0.778x_B - 1.11x_C + 0.111 = 0$	1, 3, 4
$17.0x_A + 12.9x_B + 10.0x_C - 9.00 = 0$	2, 4, 5
$12.9x_A + 17.0x_B + 10.0x_C - 9.00 = 0$	3, 4, 5

Equations for Regions

Liquid-Liquid Envelope:

$0.778x_A - 0.329x_B - 1.11x_C + 0.111 < 0$
$-0.328x_A + 0.778x_B - 1.11x_C + 0.111 < 0$
$17.0x_A + 12.9x_B + 10.0x_C - 9.00 < 0$
$12.9x_A + 17.0x_B + 10.0x_C - 9.00 < 0$

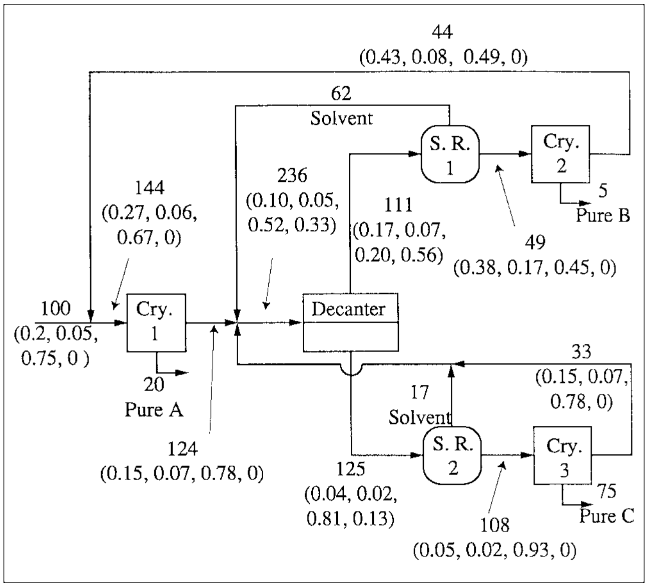

Figure 9. Flowsheet for separating a quaternary mixture with crystallization and decantation.

common boundary points. For simplicity, all tie lines for this envelope are assumed to pass through pure C—or the composition (0, 0, 1, 0) and can be determined by joining the overall composition and (0, 0, 1, 0) with Eqs. 3 to 5. A tie line then intersects two of the boundaries of the liquid-liquid envelope, producing two product streams.

A feasible flowsheet is displayed in Figure 9. Pure A is crystallized from the feed in the first crystallizer. The mother liquor is mixed with two recycle streams and sent to the decanter. At the decanter temperature, a liquid-liquid split produces a C lean phase and a C rich phase. The C lean phase is sent to the first solvent recovery unit, which recycles solvent S back to the decanter. The rest is fed to crystallizer 2. This crystallizer recovers pure B; the mother liquor is recycled back to the first crystallizer. The C rich stream from the decanter is fed to the second solvent removal unit. This unit provides an additional solvent recycle back to the decanter and a feed stream for the third crystallizer. The third crystallizer recovers pure C and produces a mother liquor stream, which is also recycled back to the decanter.

Conclusions

Separation system synthesis is a diverse and complex subject. Considerable progress has been made towards applications in specific technologies and the unifying principles. This work views separation as movements in composition space. Beginning with a feed composition and flow rate, we step through the composition space to reach the specified product compositions.

The definition of the composition space depends on the separation technique under consideration. Crystallization path maps and residue curve maps are well-known examples. It also depends on the mode of operation. For example, a polythermal phase diagram should be used for cooling crystallization and an isothermal phase diagram should be used for evaporative crystallization. The dimension of the composition space also changes. To separate an n-component mixture, the dimension is greater than n if separating agents are used and its dimensionality decreases as pure components are completely removed from the mixture.

The journey through the composition spaces can be blocked by the presence of process boundaries due to thermodynamic boundaries caused by eutectics, azeotropes, or immiscibility gaps, or due to equipment boundaries caused by the properties of the solid-phase separating agents. In order to bypass these boundaries so as to reach the specified product compositions, we select, combine and configure various separation techniques to form a hybrid separation system using heuristics available in the literature.

Representing a composition space with a dimension of four or higher can be difficult. A method is proposed to identify the regions, boundaries, as well as all the lower dimensional varieties in an N-dimensional space. The accompanying synthesis procedure can rely entirely on calculations although lower dimensional systems can be graphically depicted. To facilitate the synthesis calculations, a process boundary is approximated as a linear hyperplane if appropriate, while a nonlinear boundary is represented using a set of linear hyperplanes.

It should be emphasized that the use of this easy-to-implement, user-driven process boundary-based approach does not require complete knowledge of all the composition spaces in their entirety. For the chosen separation technique, only the region of the composition space corresponding to the stream to be separated needs to be considered. It also does not require theoretical prediction of the fixed points or boundaries; experimental data can be entered into the calculational procedure in the spreadsheet. Indeed, as illustrated with examples in O'Young et al. (1997), this boundary approach can help focus our attention on the useful part of the phase diagrams and thus minimize the amount of data necessary for separation system synthesis. Further work is underway to integrate this approach to separation task selection so as to expedite the generation of flowsheet alternatives.

Acknowledgment

Financial support in the form of a National Science Foundation Fellowship awarded to T.G.P. is gratefully acknowledged. We thank L. O'Young and M. F. Doherty for helpful discussions on this work.

Notation

a_{ij} = constant parameter
b = constant parameter
$g_i(x)$ = boundary i as a function of the compositions x
$g(x)$ = vector function containing all of the boundaries for a composition space, where each element is a boundary
t = variable parameter
t_i = variable parameter
x_i^j = composition of component i in stream j
x^j = composition vector of stream j
α = membrane separation factor
θ = membrane cut

Literature Cited

Ahmad, B. S., and P. I. Barton, "Homogeneous Multicomponent Azeotropic Batch Distillation," *AIChE J.*, **42**, 3419 (1996).

Ahmad, B. S., Y. Zhang, and P. I. Barton, "Product Sequences in

Azeotropic Batch Distillation," *AIChE J.*, **44**, 1051 (1998).

Barnicki, S. D., and J. R. Fair, "Separation System Synthesis: A Knowledge-Based Approach. 1. Liquid Mixture Separations," *Ind. Eng. Chem. Res.*, **29**, 421 (1990).

Barnicki, S. D., and J. R. Fair, "Separation System Synthesis: A Knowledge-Based Approach. 2. Gas/Vapor Mixtures," *Ind. Eng. Chem. Res.*, **31**, 1679 (1992).

Barnicki, S. D., and J. J. Siirola, "Separations Process Synthesis," *Encyclopedia of Chemical Technology*, 4th ed., Vol. 21, Wiley, New York, p. 923 (1997).

Berry, D. A., "Conceptual Design of Crystallization-Based Separation Processes," PhD Thesis, Univ. of Massachusetts, Amherst (1997).

Berry, D. A., and K. M. Ng, "Separation of Quaternary Conjugate Salt Systems by Fractional Crystallization," *AIChE J.*, **42**, 2162 (1996).

Berry, D. A., and K. M. Ng, "Synthesis of Reactive Crystallization Processes," *AIChE J.*, **43**, 1737 (1997a).

Berry, D. A., and K. M. Ng, "Synthesis of Crystallization-Distillation Hybrid Separation Processes," *AIChE J.*, **43**, 1751 (1997b).

Berry, D. A., S. R. Dye, and K. M. Ng, "Synthesis of Drowning-Out Crystallization-Based Separations," *AIChE J.*, **43**, 91 (1997).

Brunet, J. C., and Y. A. Liu, "Studies in Chemical Process Design and Synthesis. 10. An Expert System for Solvent-Based Separation Process Synthesis," *Ind. Eng. Chem. Res.*, **32**, 315 (1993).

Cisternas, L. A., and D. F. Rudd, "Process Designs for Fractional Crystallization from Solution," *Ind. Eng. Chem. Res.*, **32**, 1993 (1993).

Douglas, J. M., "Synthesis of Separation System Flowsheets," *AIChE J.*, **41**, 2522 (1995).

Douglas, P. L., M. K. Garg, J. G. Linders, and S. K. Mallick, "A New Algorithm for Selection of Separation Technologies," *Trans. IChemE*, **71**, Part A, 479 (1993).

Dye, S. R., and K. M. Ng, "Bypassing Eutectics with Extractive Crystallization: Design Alternatives and Tradeoffs," *AIChE J.*, **41**, 1456 (1995a).

Dye, S. R., and K. M. Ng, "Fractional Crystallization: Design Alternatives and Tradeoffs," *AIChE J.*, **41**, 2427 (1995b).

Fien, G. A. F., and Y. A. Liu, "Heuristic Synthesis and Shortcut Design of Separation Processes Using Residue Curve Maps: A Review," *Ind. Eng. Chem. Res.*, **33**, 2505 (1994).

Gani, R., and L. Constantinou, "Molecular Structure Based Estimation of Properties for Process Design," *Fluid Phase Equilibria*, **116**, 75 (1996).

Jaksland, C. A., R. Gani, and K. M. Lien, "Separation Process Design and Synthesis Based on Thermodynamic Insights," *Chem. Eng. Sci.*, **50**, 511 (1995).

Malone, M. F., and M. F. Doherty, "Separation System Synthesis for Nonideal Liquid Mixtures," *AIChE Symp. Ser.*, **91**, 9 (1995).

Mizsey, P., and Z. Fonyo, "Toward a More Realistic Overall Process Synthesis—The Combined Approach," *Computers Chem. Eng.*, **14**, 1213 (1990).

O'Young, L., Y. Natori, T. G. Pressly, and K. M. Ng, "A Physical Limitation Based Framework for Separations Synthesis," *Comp. Chem. Eng.*, **21**, S223 (1997).

Pressly, T. G., and K. M. Ng, "A Break-Even Analysis of Distillation-Membrane Hybrids," *AIChE J.*, **44**, 93 (1998).

Qian, Y., and K. M. Lien, "Rule Based Synthesis of Separation Systems by Predictive Best First Search with Rules Represented as Trapezoidal Numbers," *Computers Chem. Eng.*, **19**, 1185 (1995).

Rooks, R. E., "Feasibility and Column Sequencing for the Distillation of Homogeneous Multicomponent Azeotropic Mixtures," PhD Thesis, University of Massachusetts, Amherst (1997).

Safrit, B. T., and A. W. Westerberg, "Algorithm for Generating the Distillation Regions for Azeotropic Multicomponent Mixtures," *Ind. Eng. Chem. Res.*, **36**, 1827 (1997).

Siirola, J. J., "Strategic Process Synthesis: Advances in the Hierarchical Approach," *Computers Chem. Eng.*, **20**, S1637 (1996).

Wahnschafft, O. M., T. P. Jurain, and A. W. Westerberg, "Split: A Separation Process Designer," *Computers Chem. Eng.*, **15**, 565 (1991).

Widagdo, S., and W. D. Seider, "Azeotropic Distillation," *AIChE J.*, **42**, 96 (1996).

Manuscript received Mar. 27, 1998, and revision received Jan. 14, 1999.